

Di- and Tetranuclear Metal Complexes with Phenoxo Bridges: Synthesis, Structures, and Photoluminescent and Electroluminescent Properties

Hong-Yu Zhang, Kai-Qi Ye, Jing-Ying Zhang, Yin Liu, and Yue Wang*

Key Laboratory for Supramolecular Structure and Materials of Ministry of Education, College of Chemistry, Jilin University, Changchun 130012, People's Republic of China

Received September 8, 2005

Dinuclear and tetranuclear copper 2,6-bis(2-hydroxyphenyl)pyridine (H₂L) complexes Cu₂(L)₂(py)₂ (**1**) and Cu₄(L)₄(DMF) (**2**) were synthesized. The complexes **1** and **2** were characterized by elemental analyses, mass spectrometry, and single-crystal X-ray diffraction analyses. **1** crystallizes in the monoclinic space group *P2₁/n* with *a* = 13.330(2) Å, *b* = 9.361(1) Å, *c* = 14.676(1) Å, *β* = 100.94(1)°, *V* = 1798.1(3) Å³, and *Z* = 2. **2** crystallizes in the monoclinic space group *P2₁/n* with *a* = 13.360(1) Å, *b* = 14.884(1) Å, *c* = 15.462(2) Å, *β* = 97.50(4)°, *V* = 3048.4(1) Å³, and *Z* = 2. Tetranuclear zinc complex Zn₄(L)₄(py)₄ (**3**) was prepared and characterized by X-ray diffraction. **3** crystallizes in the triclinic space group *P $\bar{1}$* with *a* = 13.770(1) Å, *b* = 15.465(1) Å, *c* = 16.409(2) Å, *α* = 88.877(9)°, *β* = 88.035(4)°, *γ* = 82.956(3)°, *V* = 3465.6(5) Å³, and *Z* = 2. The di- and tetranuclear complexes **1**–**3** contain phenoxo bridges. **1** is a dinuclear complex with two Cu(II) centers, two py ligands, and two L ligands, and each L ligand donates its pyridyl ring and one of the phenolate groups to one metal and shares the other phenolate group between both metals, affording a Cu₂(μ-O)₂ core. **2**, in contrast, is a tetranuclear complex with four Cu(II) centers and four L ligands. Two of the L ligands have the same coordination mode as **1**, and the other two L ligands donate their pyridyl rings to one metal and share both phenolate groups between four metals, resulting in three four-membered Cu₂(μ-O)₂ rings, which joined each other and showed great distortion from planarity. **3** is a tetranuclear complex with four Zn(II) centers, four pyridine ligands, and four L ligands, and the L ligands have the same coordination modes as those of **2**. Single-crystal X-ray analysis showed that hydrogen-bonding and π–π stacking interactions exist in complexes **1** and **2** resulting in two- and three-dimensional molecular arrangements, and the parallel arrangement of the ligand in the crystal of complex **3** resulted in a close inter- and intramolecular π–π interactions. Investigation of the crystals, as well as an amorphous thin film and powder of **3**, by photoluminescence (PL) allowed the effect of the molecular packing on the emission properties to be elucidated. Furthermore, the electroluminescent (EL) properties of **3** were examined by fabricating a multilayer device with structure of [ITO/NPB/(ZnL)_{*n*}/Alq₃/LiF/Al] (NPB = *N,N'*-bis(α-naphthyl)-*N,N'*-diphenyl-(1,1'-biphenyl)-4,4'-diamine, Alq₃ = tris(8-hydroxyquinolinato)aluminum).

Introduction

Polypyridines are widely used as polydentate chelating ligands that play a major role in the current intense interest in coordination chemistry. The coordination chemistry of polydentate chelating ligands which contain mixed pyridine–phenol donor sets has been a very popular target of study and is one of possible extension to the chemistry of polypyridines. Ward and co-workers developed early studies

of the complexes based on the mixed-donor polydentate ligands.^{1–4} We have demonstrated that the mixed phenol–pyridine ligands could be used to develop new blue electroluminescent (EL) materials.^{5,6} We have also reported white light emission which comes from exciplex from phenol–

- (1) Jeffery, J. C.; Schatz, E.; Ward, M. D. *J. Chem. Soc., Dalton Trans.* **1992**, 1921.
- (2) Holligan, B. M.; Jeffery, J. C.; Norgett, M. K.; Schatz, E.; Ward, M. D. *J. Chem. Soc., Dalton Trans.* **1993**, 2321.
- (3) Jeffery, J. C.; Thornton, P.; Ward, M. D. *Inorg. Chem.* **1994**, *33*, 3612.
- (4) Holligan, B. M.; Jeffery, J. C.; Norgett, M. K.; Schatz, E.; Ward, M. D. *J. Chem. Soc., Dalton Trans.* **1992**, 3345.

* To whom correspondence should be addressed. E-mail: yuewang@jlu.edu.cn. Fax: +86-431-5193421.

pyridine boron complexes.^{7,8} The terminal phenolate residues of these ligands are capable of bridging two metal ions, allowing the formation of dinuclear⁹ and tetranuclear⁴ phenolate-bridged complexes. The use of different bridging ligands and well-designed polydentate ligands has afforded an impressive array of polynuclear coordination complexes. The resulting complexes have been proved to be interesting for a variety of reasons. Moreover, some unusual structures for copper(II) and nickel(II) complexes have been established in which noncovalent interactions such as hydrogen bonding and π - π stacking appear to play a dominant part.^{1,10,11} When the denticity of the ligand has vacant coordination sites at the metal ions, these sites are saturated under certain circumstances by self-assembly to polynuclear arrays, often in the presence of additional bridging groups such as alkoxo or phenoxo oxygen atoms. So a considerable degree of control can be exerted over the self-assembly process by judicious choice of components such that the number, denticity, and disposition of the binding sites in the ligand and the coordination number and geometric preferences of the metal ions can precisely be matched to a remarkable degree of specificity in the self-assembly process.¹²⁻¹⁹ In particular, the coordinatively flexible Cu(II) and Zn(II) permit a wide variety of structural arrangements. Motivated by the success of tris(8-hydroxyquinolino)aluminum (Alq₃) in vacuum-deposited LEDs, organic chelate metal complexes have in particular attracted a lot of attention.²⁰⁻²⁴ Yu and co-workers have carefully studied the molecular and elec-

tronic structures and electron transport properties in LEDs based on the dinuclear zinc complex [Zn(BTZ)₂]₂.²³ Sapochak and co-workers have reported structural effects of the tetranuclear zinc complex (Znq₂)₄ on electronic states and device performance.²⁴

In this paper, we report the synthesis, characterization, and crystal structures of three novel dinuclear and tetranuclear Cu(II) and Zn(II) complexes. As a continuation of our interest in the investigation of mixed phenol-pyridyl ligands, H₂L was chosen as a bridging ligand to construct novel polynuclear complexes **1-3**, which have been characterized by X-ray diffraction analysis. The PL and EL properties of **3** are studied.

Experimental Section

Materials and General Methods. All the reagents for syntheses were commercially available and used without further purification. 2,6-Dibromopyridine (Fluka), 2-bromoanisole (Fluka), and LiF (Aldrich) were used as received. Alq₃ was purchased from Aldrich and purified by vacuum sublimation. *N,N'*-Bis(α -naphthyl)-*N,N'*-diphenyl-(1,1'-biphenyl)-4,4'-diamine (NPB)²⁵ and 2,6-bis(2-hydroxyphenyl)pyridine (H₂L)⁶ were synthesized according to the literature procedures.

Instrumentation. ¹H NMR spectra were recorded on Bruker AVANVE 500 MHz spectrometer with tetramethylsilane as the internal standard. Mass spectra were recorded on a GC/MS mass spectrometer. UV-vis absorption spectra were determined on a PE UV-vis Lambda spectrometer. The emission spectra were recorded with a Shimadzu RF-5301 PC spectrometer. Elemental analyses were performed on a flash EA 1112 spectrometer. The EL spectra, luminance, and CIE coordinates of the device were recorded on a PR650 spectrometer.

Photoluminescence (PL) and Electroluminescence (EL) Measurements. The device was built on glass that was precoated with ITO. The ITO glass was routinely cleaned by ultrasonic treatment in detergent solutions, rinsed with acetone, boiled in isopropyl alcohol, and rinsed with methanol and then with deionized water. The glass was dried in a vacuum oven between each cleaning step. The devices were fabricated by successive vacuum deposition of organic materials onto the ITO-coated glass substrate. Prior to deposition, all organic materials were purified by sublimation. A shadow mask with 2 × 3 mm² openings was used to define the cathodes. Luminance-voltage and current-voltage characteristics were measured at room temperature under ambient atmosphere. Crystals, powder, and solid thin film deposited on a quartz substrate of complex **3** were employed to record the fluorescence spectra.

2,6-Bis(2-hydroxyphenyl)pyridine (H₂L). A solution of the Grignard reagent prepared from 2-bromoanisole (6.0 g, 30 mmol) was added dropwise to an ice-cold mixture of Ni(dppe)Cl₂ (dppe = Ph₂PCH₂CH₂PPh₂) (0.52 g, 1 mmol) and 2,6-dibromopyridine (3.6 g 15 mmol) in dry tetrahydrofuran (THF 40 mL) under N₂. The mixture was stirred at room temperature for 12 h and then quenched with aqueous NH₄Cl, and THF was removed under reduced pressure. The resulting white precipitate was filtered off, washed with water, and dried in air to give 1,6-bis(2-methoxyphenyl)pyridine, which was used directly in the subsequent step without further purification. 1,6-Bis(2-methoxyphenyl)pyridine was added to molten pyridinium chloride (from 40 mL of pyridine and 45 mL of concentrated HCl) under N₂ over 3 h at 200 °C. After

- (5) Li, Y. Q.; Liu, Y.; Bu, W. M.; Lu, D.; Wu, Y.; Wang, Y. *Chem. Mater.* **2000**, *12*, 2672.
- (6) Li, Y. Q.; Liu, Y.; Bu, W. M.; Guo, J. H.; Wang, Y. *Chem. Commun.* **2000**, 1551.
- (7) Feng, J.; Li, F.; Gao, W. B.; Liu, S. Y.; Liu, Y.; Wang, Y. *Appl. Phys. Lett.* **2001**, *78*, 3497.
- (8) Liu, Y.; Guo, J. H.; Zhang, H. D.; Wang, Y. *Angew. Chem., Int. Ed.* **2002**, *41*, 182.
- (9) Maher, J. P.; Rieger, P. H.; Thornton, P.; Ward, M. D. *J. Chem. Soc., Dalton Trans.* **1992**, 3353.
- (10) Jeffery, J. C.; Ward, M. D. *J. Chem. Soc., Dalton Trans.* **1992**, 2119.
- (11) Holligan, B. M.; Jeffery, J. C.; Ward, M. D. *J. Chem. Soc., Dalton Trans.* **1992**, 3331.
- (12) Garcia, A. M.; Bassani, D. M.; Lehn, J. M.; Baum, G.; Fenske, D. *Chem.-Eur. J.* **1999**, *5*, 1234.
- (13) Hanan, G. S.; Volmer, D.; Schubert, U. S.; Lehn, J. M.; Baum, G.; Fenske, D. *Angew. Chem., Int. Ed. Engl.* **1997**, *36*, 1842.
- (14) Piguet, C.; Hopfgartner, G.; Williamsand, A. F.; Bünzli, J. C. G. *J. Chem. Soc., Chem. Commun.* **1995**, 2575.
- (15) Piguet, C.; Minten, E. R.; Bernardinelli, G.; Bünzli, J.-C. G.; Hopfgartner, G. *J. Chem. Soc., Dalton Trans.* **1997**, 421.
- (16) Fujita, M. *Chem. Soc. Rev.* **1998**, *27*, 417.
- (17) Takeda, N.; Umemoto, K.; Yamaguchi, K.; Fujita, M. *Nature (London)* **1999**, *398*, 794.
- (18) Olenyuk, B.; Whiteford, J. A.; Fechtenkötner, A.; Stang, P. J. *Nature (London)* **1999**, *398*, 796.
- (19) Stang, P. J.; Olenyuk, B. *Acc. Chem. Res.* **1997**, *30*, 502.
- (20) Hopkins, T. A.; Meerholz, K.; Shaheen, S.; Anderson, M. L.; Schmidt, A.; Kippelen, B.; Padias, A. B.; Hall, K. K., Jr.; Peyghambarian, N.; Armstrong, N. R. *Chem. Mater.* **1996**, *8*, 344.
- (21) Sapochak, L. S.; Padmaperuma, A.; Washton, N.; Endrino, F.; Schmett, G. T.; Marshall, J.; Fogarty, D.; Burrows, P. E.; Forrenst, S. R. *J. Am. Chem. Soc.* **2001**, *123*, 6300.
- (22) Wang, J. F.; Wang, R. Y.; Yang, J.; Zheng, Z. P.; Carduct, M. D.; Cayou, T.; Peyghambarian, N.; Jabbour, G. E. *J. Am. Chem. Soc.* **2001**, *123*, 6179.
- (23) Yu, G.; Yin, S. W.; Liu, Y. Q.; Shuai, Z. G.; Zhu, D. B. *J. Am. Chem. Soc.* **2003**, *125*, 14816.
- (24) Linda, S. S.; Floerfida, E.; Benicasa, Richard, S.; Schofield, Joseph L. B.; Krystal, K. C.; Riccio, D. F.; Holger, K.; Kim, F. Ferris.; Paul, E. B. *J. Am. Chem. Soc.* **2002**, *124*, 6119.

- (25) Koren, A. B.; Curtis, M. D.; Kampf, J. W. *Chem. Mater.* **1998**, *10*, 2235.

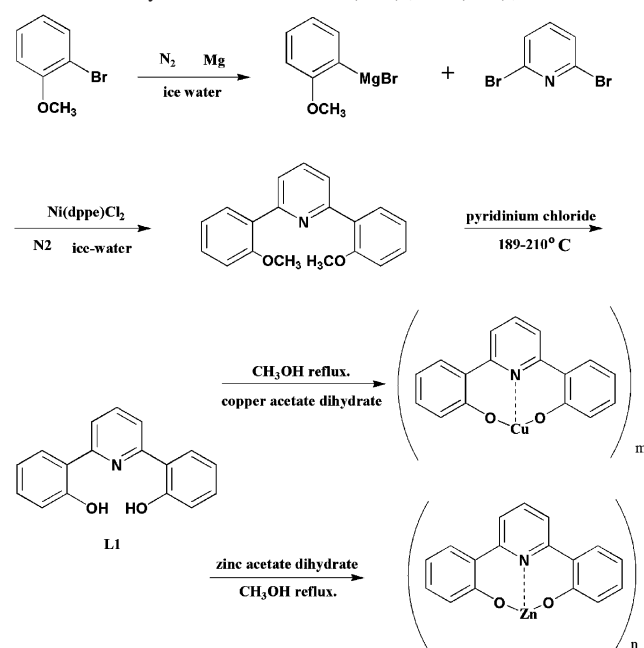
Table 1. X-ray Crystallographic Data for 1–3

param	identification code		
	1	2	3
empirical formula	C ₄₄ H ₃₂ Cu ₂ N ₄ O ₄	C ₇₄ H ₅₈ Cu ₄ N ₆ O ₁₀	C ₁₇ H ₁₃ NO ₈ Zn ₄
fw	807.82	1445.42	1622.95
temp (K)	293(2)	293(2)	293(2)
cryst system, space group	monoclinic, <i>P</i> 2 ₁ / <i>n</i>	monoclinic, <i>P</i> 2 ₁ / <i>n</i>	triclinic, <i>P</i> $\bar{1}$
unit cell dimens (Å, deg)	<i>a</i> = 13.330(2) <i>b</i> = 9.3612(9) <i>c</i> = 14.676(1) β = 100.941(9)	<i>a</i> = 13.360(3) <i>b</i> = 14.884(3) <i>c</i> = 15.462(3) β = 97.50(3)	<i>a</i> = 13.7700(10) <i>b</i> = 15.4649(15) <i>c</i> = 16.4093(16) α = 88.877(9) β = 88.035(4) γ = 82.956(3)
<i>V</i> (Å ³)	1798.1(3)	3048.4(11)	3465.6(5)
<i>Z</i>	2	2	2
calcd density (g/cm ³)	1.492	1.575	1.417
<i>F</i> (000)	828	1480	1512
θ range for data collcn (deg)	2.29–25.00	1.90–27.48	1.24–27.48
limiting indices	$-1 \leq h \leq 8$ $-1 \leq k \leq 11$ $-17 \leq l \leq 17$	$0 \leq h \leq 17$ $0 \leq k \leq 19$ $-20 \leq l \leq 19$	$0 \leq h \leq 17$ $-19 \leq k \leq 19$ $-21 \leq l \leq 21$
reflcn collcd/unique	4821/2108 (<i>R</i> _{int} = 0.0535)	6884/424 (<i>R</i> _{int} = 0.0912)	18 790/14 617 (<i>R</i> _{int} = 0.0777)
refinement method	full-matrix least-squares on <i>F</i> ²	full-matrix least-squares on <i>F</i> ²	full-matrix least-squares on <i>F</i> ²
data/restraints/params	2108/0/308	6884/0/424	14617/0/973
goodness-of-fit on <i>F</i> ²	1.042	0.796	1.029
final <i>R</i> indices [<i>I</i> > 2σ(<i>I</i>)]	<i>R</i> ₁ = 0.0392, <i>wR</i> ₂ = 0.0781	<i>R</i> ₁ = 0.0561, <i>wR</i> ₂ = 0.1190	<i>R</i> ₁ = 0.0838, <i>wR</i> ₂ = 0.2591
<i>R</i> indices (all data)	<i>R</i> ₁ = 0.0662, <i>wR</i> ₂ = 0.0879	<i>R</i> ₁ = 0.1540, <i>wR</i> ₂ = 0.1585	<i>R</i> ₁ = 0.1248, <i>wR</i> ₂ = 0.2801
largest diff peak/hole (e ⁻ Å ⁻³)	0.341 and -0.319	0.721 and -1.271	1.298 and -1.333

addition of water to the mixture and neutralization with aqueous KOH, the crude product was extracted with CH₂Cl₂ (3 × 60 mL). The organic phase was washed with water (2 × 30 mL) and dried over Na₂SO₄. The solvent was removed under reduced pressure, giving the residual white powder in 55% yield. ¹H NMR (CDCl₃): δ = 8.11–8.90 (2 H, s), 8.00 (1 H, t, *J* = 8.0 Hz), 7.72 (2 H, d, *J* = 8.0 Hz), 7.68 (2 H, d, *J* = 8.0 Hz), 7.35 (2 H, t, *J* = 8.0 Hz), 7.06 (2 H, d, *J* = 8.0 Hz), 7.01 (2 H, t, *J* = 7.5 Hz). MS: *m/z* 263, [M]⁺. Anal. Calcd for C₁₇H₁₃NO₂: C, 77.55; H, 4.98; N, 12.15. Found: C, 77.36; H, 4.75; N, 12.31.

Cu₂(L)₂(py)₂ (1) and Cu₄(L)₄(DMF) (2). A solution of 2,6-bis(2-hydroxyphenyl)pyridine (H₂L) dissolved in 30 mL of CHCl₃ was added dropwise to a solution of copper acetate dihydrate in CH₃-OH. The resultant green solution was stirred for 1 h at room temperature, and then 1.5 mL of Et₃N was added resulting in the formation of green precipitate, which was filtered off and dried in a vacuum. X-ray-quality crystals of **1** were obtained by slow diffusion of diethyl ether vapor into a pyridine solution of the green solid. MS: *m/z* 806, [M]⁺. Anal. Calcd for C₄₄H₃₂Cu₂N₄O₄: C, 65.42; H, 3.99; N, 6.94. Found: C, 65.21; H, 4.15; N, 6.81. X-ray-quality crystals of **2** were grown by slow diffusion of diethyl ether vapor into a DMF solution of the green solid. MS: *m/z* 1442, [M]⁺. Anal. Calcd for C₇₄H₅₈Cu₄N₆O₁₀: C, 61.49; H, 4.04; N, 5.81. Found: C, 61.28; H, 4.19; N, 5.78.

Zn₄(L)₄(py)₄ (3). A solution of 2,6-bis(2-hydroxyphenyl)pyridine (H₂L) dissolved in 30 mL of CHCl₃ was added dropwise to a solution of zinc acetate dihydrate in CH₃OH. The resultant green solution was stirred at room temperature for 1 h, whereupon dropwise addition of aqueous Et₃N (1.5 mL) precipitated a white solid, which was filtered off and dried in a vacuum. The compound was not characterized by mass spectrometry and ¹H NMR spectroscopy because of the poor solubility. Elemental analysis revealed that the formula composition of the white solid was (ZnL)_{*n*}. Anal. Calcd for (ZnL)_{*n*}: C, 62.51; H, 3.39; N, 4.29. Found: C, 62.69; H, 3.32; N, 4.17. Single crystals of **3** suited for X-ray structural analysis were grown by slow diffusion of diethyl ether vapor into a pyridine solution of the white solid. MS: *m/z* 1616, [M]⁺. Anal. Calcd for C₈₈H₆₄Zn₄N₈O₈: C, 65.12; H, 3.97; N, 6.90. Found: C, 65.21; H, 3.79; N, 6.81.

Scheme 1. Synthesis Procedure for (CuL)_{*m*} and (ZnL)_{*n*}

X-ray Diffraction. X-ray diffraction data for **1** were collected on a Siemens R³ four-circle diffractometer using graphite-monochromated Mo K α radiation and ω -scans at room temperature. X-ray diffraction data for **2** and **3** were collected on a Rigaku RAXIS-PRID diffractometer using the ω -scan technique with graphite-monochromated Mo K α (λ = 0.0710 73 Å) radiation. The structures were solved with direct methods and refined with the full-matrix least-squares technique, using the SHELXTL programs. Anisotropic displacement parameters were applied to all non-hydrogen atoms. Hydrogen atoms were assigned isotropic displacement coefficients. Crystal data as well as details of data collection and refinement for the complexes **1–3** are summarized in Table 1.

Results and Discussion

Syntheses. Synthesis of the ligand H₂L was accomplished according to the method outlined in Scheme 1. The reactions

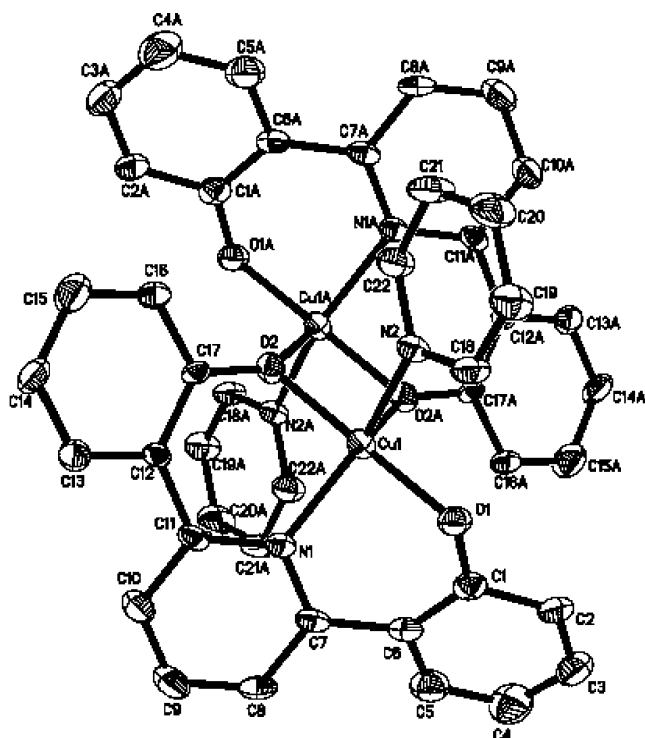


Figure 1. ORTEP views of **1** (30% probability displacement ellipsoids) with the atom-numbering scheme and with hydrogen atoms having been omitted for clarity.

Table 2. Selected Bond Lengths (Å) and Angles (deg) for **1**^a

Cu(1)—O(1)	1.895(3)	Cu(1)—O(2) ^{#1}	2.257(2)
Cu(1)—O(2)	1.929(3)	Cu(1)—N(2)	2.061(4)
Cu(1)—N(1)	2.016(4)		
O(1)—Cu(1)—O(2)	177.3(1)	N(1)—Cu(1)—N(2)	147.7(1)
O(1)—Cu(1)—N(1)	91.0(2)	O(1)—Cu(1)—O(2) ^{#1}	101.6(1)
O(2)—Cu(1)—N(1)	89.2(2)	O(2)—Cu(1)—O(2) ^{#1}	75.9(1)
O(1)—Cu(1)—N(2)	88.9(2)	N(1)—Cu(1)—O(2) ^{#1}	109.3(1)
O(2)—Cu(1)—N(2)	92.3(2)	N(2)—Cu(1)—O(2) ^{#1}	102.3(1)

^a Symmetry codes: (#1) $-x + 2, -y, -z + 1$.

of copper acetate and zinc acetate with 1 equiv of H₂L in methanol quickly gave a dark green solution and a yellow green solution, from which a green solid and white solid were precipitated by addition of Et₃N, respectively, and recrystallized from pyridine–diethyl ether and DMF–diethyl ether, leading to three different polynuclear complexes **1–3**.

Molecular Structures. The structure determination revealed that two copper atoms Cu(1) and Cu(1A) are bridged by phenoxo in **1**. A perspective view with atom-numbering scheme of **1** is shown in Figure 1. Selected bond distances and angles of complex **1** are summarized in Table 2. The centrosymmetric cation is built up of a pyridine ligand and a L ligand that bridge a pair of Cu atoms at a distance of 3.308 Å with bridging angle [Cu(1)—O(2)—Cu(1A) = 104.1-(2)°] through the deprotonated phenolate oxygen atoms, forming two CuN₂O₂ polyhedron that joined their shared vertex by the oxygen atom of the phenoxo bridging in a face-to-face fashion. The two L ligands, which obviously are structurally equivalent in the molecule, have virtually identical conformations. The L ligand is considerably distorted from planarity, and there are inter-ring torsion angles of 29.12 and 31.33°, respectively. Cu(1) is coordinated to two

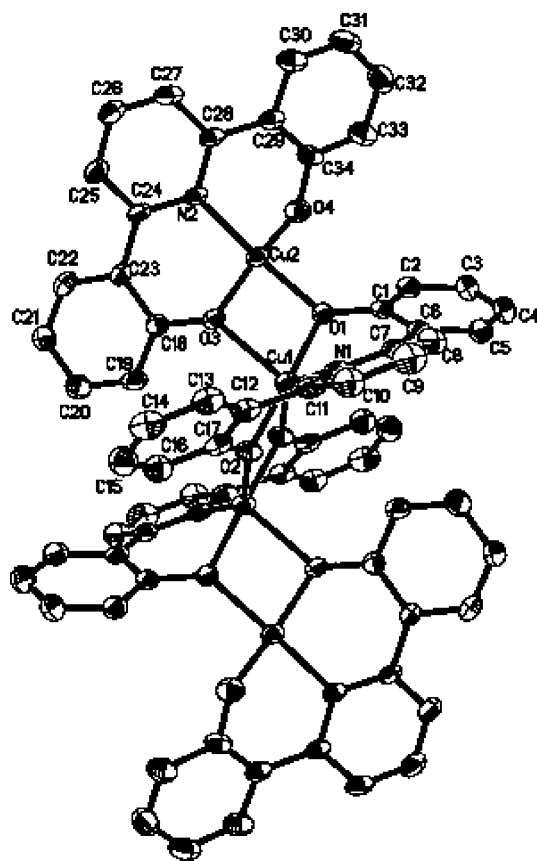


Figure 2. ORTEP views of **2** (30% probability displacement ellipsoids) with the atom-numbering scheme and with the DMF molecule and hydrogen atoms having been omitted for clarity.

phenolate oxygen atoms and two pyridine nitrogen atoms, and the fifth coordinate site of Cu(1) is occupied by the phenolate oxygen of the other ligand bridging Cu(1) and Cu(1A). The whole molecule is related by a center of inversion. The Cu—O distances show significant differences [Cu(1)—O(1) = 1.895(3) Å, Cu(1)—O(2) = 1.929(3) Å] that should be attributed to the Cu(1)—O(2)—Cu(1A) bridge coordination geometry.²⁶ The coordination environment of Cu is best described as distorted trigonal-bipyramidal. For the Cu(1) center, N(1) and N(2) occupy the axial positions with the angle of N(1)—Cu(1)—N(2) = 147.7(1)° and O(1), O(2), and O(2A) atoms are in the trigonal plane.

2 can be described as a centrosymmetric tetranuclear complex (Figure 2). The selected bond lengths and angles are given in Table 3. **2** consists of two identical dinuclear Cu₂(L)₂ subunits which connect to each other via the coordination of the dangling phenolate oxygen atoms. Two copper ions within a subunit are bridged by two phenolate oxygen atoms. The tetranuclear core consists of two dinuclear Cu₂(L)₂ units, in which the L ligand is tridentate and deprotonated, stacked adjacent to one another such that the phenolates bridge the copper centers giving three four-membered Cu₂(μ-O)₂ rings, which joined each other and showed great distortion from planarity. For tetranuclear Cu₄(L)₄(DMF) the terminal copper atoms Cu(2) are four-

(26) Koner, S.; Saha, S.; Okamoto, K.-I.; Tuchagues, J.-P. *Inorg. Chem.* **2003**, *42*, 4668.

Table 3. Selected Bond Lengths (Å) and Angles (deg) for **2**^a

Cu(1)–O(2)	1.900(4)	Cu(2)–O(4)	1.836(5)
Cu(1)–O(1)	1.909(4)	Cu(2)–O(3)	1.901(4)
Cu(1)–N(1)	2.014(5)	Cu(2)–N(2)	1.976(5)
O(2)–Cu(1)–O(1)	178.3(2)	N(2)–Cu(2)–O(1)	161.1(2)
O(2)–Cu(1)–N(1)	91.0(2)	Cu(1)–O(2)–Cu(1) ^{#1}	102.0(2)
O(1)–Cu(1)–N(1)	89.7(2)	Cu(1)–O(1)–Cu(2)	105.9(2)
O(2)–Cu(1)–O(2) ^{#1}	78.0(2)	O(2) ^{#1} –Cu(1)–O(3)	104.0(2)
O(4)–Cu(2)–N(2)	92.0(2)	O(4)–Cu(2)–O(3)	166.3(2)
O(2)–Cu(1)–O(3)	103.2(2)	O(3)–Cu(2)–N(2)	95.1(2)
O(1)–Cu(1)–O(3)	75.06(16)	O(4)–Cu(2)–O(1)	96.4(2)
N(1)–Cu(1)–O(3)	114.2(2)	O(3)–Cu(2)–O(1)	80.5(2)

^a Symmetry codes: (#1) $-x - 1, -y + 1, -z$.

coordinated and the central copper atoms Cu(1) are five-coordinated, resulting in a highly distorted bipyramidal geometry. The Cu–N distances are 2.015(5) Å [Cu(1)–N(1)] and 1.976(5) Å [Cu(2)–N(2)], respectively. The Cu–O bond lengths vary from 1.836(5) Å [Cu(2)–O(4)] to 2.195(4) Å [Cu(1)–O(3)], which is in the similar range as observed in complex **1**. The two L ligands in a subunit are also distorted from planarity, with inter-ring torsion angles of 13.62 and 36.72° between the central pyridine ring and the phenolate ring in one ligand and 27.41 and 32.78° in the other. The Cu(1)–Cu(2) and Cu(1)–Cu(1A) distances are 3.108 and 3.094 Å, respectively.

3 can be described as a tetranuclear complex consisting of two identical dinuclear Zn₂(L)₂(py)₂ subunits which connect to each other via the coordination of the dangling phenolate oxygen atoms. Selected bond lengths and angles of **3** are given in Table 4. Two zinc ions within a subunit are also bridged by two phenolate oxygen atoms. There are two halves of independent Zn₄(L)₄(py)₄ molecules in the asymmetric unit of the crystal, and the structure of complex

Table 4. Selected Bond Lengths (Å) and Angles (deg) for **3**^a

Zn(1)–O(1)	1.989(5)	Zn(2)–O(3)	1.980(5)
O(1)–Zn(1) ^{#1}	2.184(5)	Zn(2)–O(2)	2.008(5)
Zn(1)–O(2)	2.022(5)	Zn(2)–O(4)	2.051(5)
Zn(1)–N(1)	2.135(6)	Zn(2)–N(4)	2.095(7)
Zn(1)–N(1)	2.196(6)	Zn(2)–N(3)	2.098(6)
Zn(1)–O(4)	2.262(5)		
O(1)–Zn(1)–O(2)	170.8(2)	O(3)–Zn(2)–N(4)	88.9(2)
O(1)–Zn(1)–O(1) ^{#1}	79.9(2)	O(2)–Zn(2)–N(4)	114.2(2)
O(2)–Zn(1)–N(3)	107.4(2)	O(3)–Zn(2)–N(3)	89.4(2)
N(2)–Zn(1)–N(1)	173.9(2)	O(1) ^{#1} –Zn(1)–O(4)	176.9(2)
O(1) ^{#1} –Zn(1)–N(1)	92.5(2)	N(1)–Zn(1)–O(4)	90.1(2)
O(1)–Zn(1)–O(4)	101.9(2)	O(3)–Zn(2)–O(4)	176.2(2)
N(2)–Zn(1)–O(4)	84.8(2)		

^a Symmetry codes: (#1) $-x + 2, -y, -z + 2$.

3 is detailed in Figure 3. The bond lengths and angles are similar between the two Zn₄(L)₄(py)₄ molecules. Each Zn₄(L)₄(py)₄ molecule contains a crystallographic inversion center. The tetranuclear core consists of two dinuclear Zn₂(L)₂(py)₂ units with two crystallographically nonequivalent zinc atoms assuming two different coordination geometries. For a Zn₂(L)₂(py)₂ unit the L ligand is tridentate and deprotonated, stacked adjacent to one another such that the phenolates bridge the zinc centers giving a set of three four-membered Zn₂(μ-O)₂ rings, which joined each other and showed little distortion from planarity. Apart from the O, O, N donor sets of L, the basal coordination geometry of each Zn(II) ion is completed by additional coordination of a pyridyl nitrogen atom. The zinc atoms Zn(2) that are found on either end of the tetrameric unit are pentacoordinate, resulting in a distort bipyramidal geometry. In contrast, the central zinc atoms Zn(1) are hexacoordinate, resulting in a highly distorted octahedral geometry. Zn(2) is coordinated to three phenolate oxygen atoms of two L ligands and two

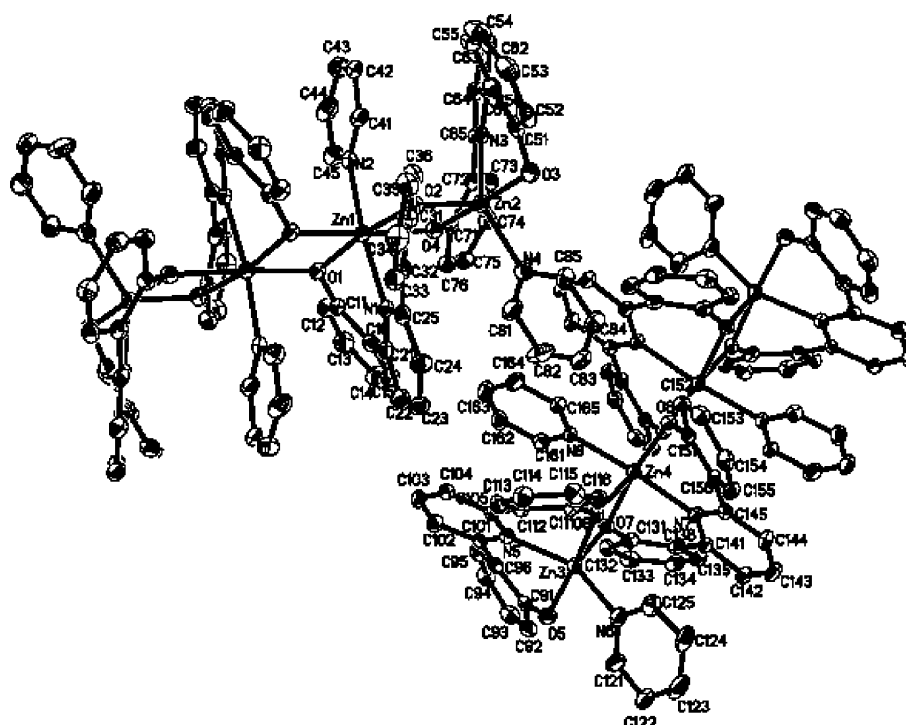


Figure 3. ORTEP views of **3** (30% probability displacement ellipsoids) with the atom-numbering scheme and with the hydrogen atoms having been omitted for clarity.

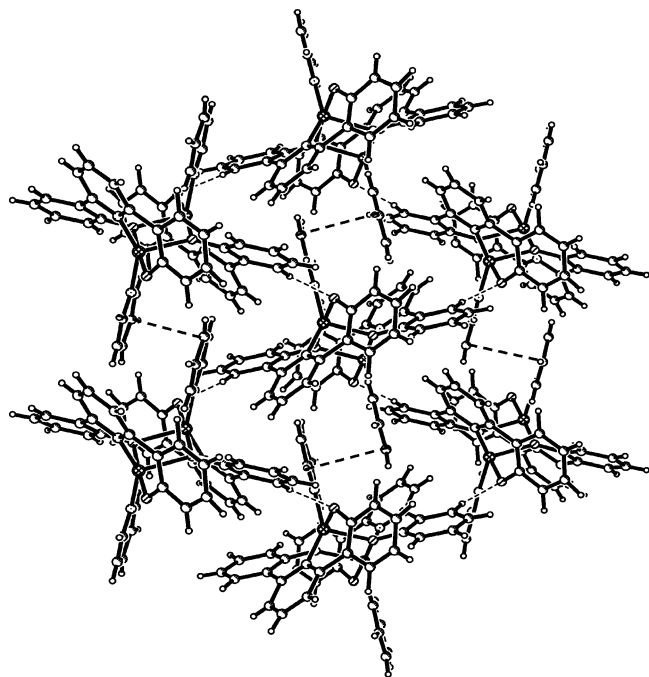


Figure 4. View along the cell *a*-axis of the hydrogen-bonded and π - π interacted molecular sheet in **1**.

pyridyl nitrogen atoms (one is from the center pyridyl atom of the L ligand and the other from the pyridine ligand), forming a ZnN_2O_3 distorted trigonal-bipyramid with O(3) and O(4) at axial positions and O(2), N(3), and N(4) in the trigonal plane. Zn(1) is coordinated to four phenolate oxygen atoms of three L ligands and two pyridyl nitrogen atoms, resulting in a ZnN_2O_4 distorted octahedral environment. Zn(1) and Zn(2) are bridged by the phenolate oxygen O(2) and O(4). The two L ligands are also distorted from planarity, with inter-ring torsion angles of 34.41° and 32.06° between the central pyridine ring and the phenolate rings in one ligand and 34.23° and 29.78° in the other. These pyridine phenolate torsion angles are comparable to those in complex **1**. The Zn(1)-Zn(2) and Zn(1)-Zn(1A) distances are 3.206 and 3.201 Å, respectively.

Molecular Packing Properties. In the solid of **1** and **2**, there exist hydrogen-bonding and π - π stacking interactions. Figure 4 shows the molecular packing feature of **1**, which extends in the crystallographic *ab* plane. Weak hydrogen-bonding interaction exists between four phenolate oxygen atoms of each $\text{Cu}_2(\text{L})_2(\text{py})_2$ molecule and four hydrogen atoms of the adjacent molecules. The structure appears to be further stabilized by aromatic π - π stacking interactions between the py ligands. The pyridine rings are nearly parallel and overlap substantially with an average interplanar separation

of 3.4 Å in the overlap region. Hydrogen-bonding and π - π stacking interactions in the crystals result in the two-dimensional infinite sheet (Figure 4). In the solid **2**, there is intermolecular π - π stacking accompanied by hydrogen-bonding interactions, which results in the formation of one-dimensional molecular chains (Figure 5). The closest interplanar distance between adjacent molecules is 3.3 Å. In solid **2** the molecular chains are held together through intermolecular hydrogen-bonding interactions between phenolate oxygen atoms and hydrogen atoms on phenyl rings (Figure 6), which results in a three-dimensional molecule arrangement. The hydrogen-bonding distances are 2.662 and 2.623 Å, respectively. In solid **3**, the parallel arrangement of the ligands on adjacent tetrameric units results in a close intermolecular π - π interaction (Figure 7a). And both the aromatic rings are almost parallel and overlap substantially with an average interplanar separation of 3.6 Å. It is noteworthy that in one of the $\text{Zn}_4(\text{ppy})_4(\text{py})_4$ units, two pyridyl rings from the L ligands and two py ligands exhibit intramolecular π - π stacking interactions (Figure 7b); however, in this case the pyridyl/pyridyl ring overlaps are weaker because of large off-plane angles between the aromatic rings. These inter- and intramolecular π - π stacking interactions occur in the crystallographic *b* direction between molecules and are one-dimensional only.

Photoluminescent (PL) and Electroluminescent (EL) Properties. The emission spectra of the crystals of **3** and solid thin film and powder of $(\text{ZnL})_n$ are presented in Figure 8. The emission of **3** in crystal form is due to the electronic π - π^* transition within the L ligand, and the spectrum is blue-shifted compared with that of solid thin film and powder. We observed that the profile of the emission spectra with a typical full width 90 nm at half-maximum (fwhm) is almost similar to those of the powder and thin film. However, the emission spectrum of the crystals is substantially blue-shifted by 60 nm with respect to those of thin film and the powder and the half-maximum (fwhm) is 55 nm. The elemental analyses indicate that the solid thin film and powder obtained by vacuum sublimation with formula of $(\text{ZnL})_n$ display a different composition compared with crystals of **3** that have the formula of $[\text{Zn}_4(\text{L})_4(\text{py})_4]$. This is maybe responsible for the difference of PL in powder and crystal states. However, it is also possible that the differences between the fluorescence spectra of crystals and powders are due to the reflections in powder because of the polycrystalline phase and the experimental setup. The L ligand conformation may be different in crystal and solid thin film or powder states. The single-crystal structure studies demon-

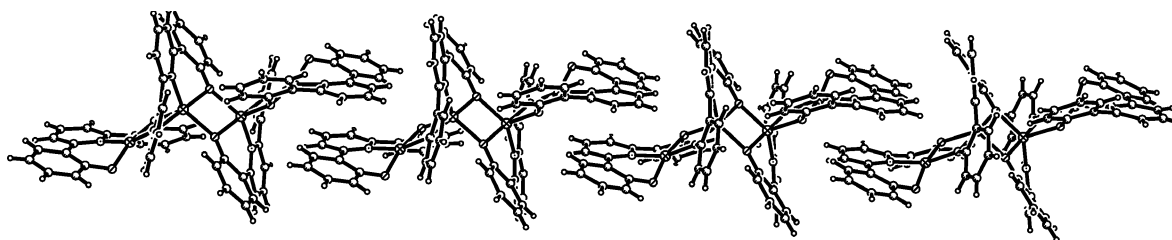


Figure 5. Crystal π - π stacking of $\text{Cu}_4(\text{L})_4$ molecules in **2**.

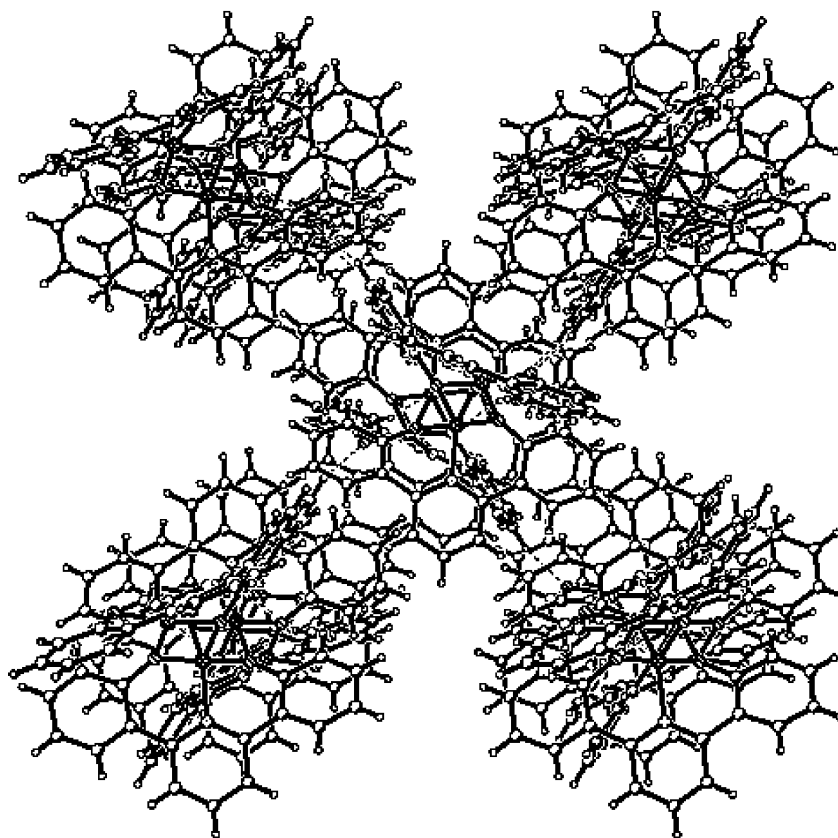


Figure 6. View of the three-dimensional structure of **2** showing molecular chains are held together through intermolecular hydrogen-bonding interactions.

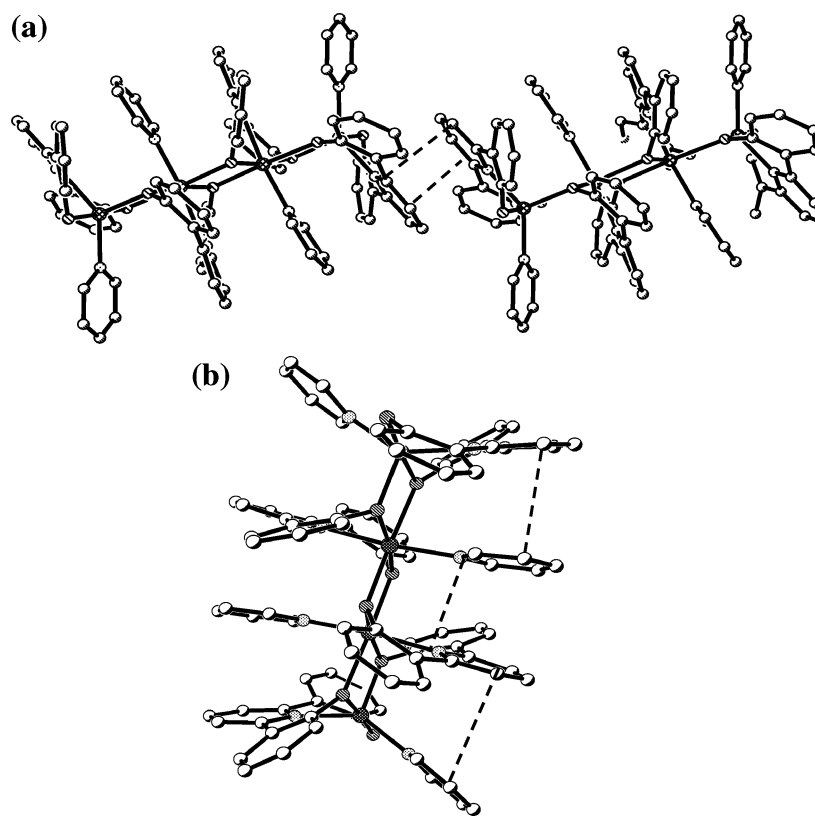


Figure 7. (a) $Zn_4(L)_4(py)_4$ molecules showing intermolecular interactions. (b) $Zn_4(L)_4(py)_4$ molecule showing intramolecular interactions.

strate that the L ligands are distorted from planarity with great torsion angles between phenolato and pyridyl rings,

which may be different in the solid thin film and powder phases. The variation of torsion angles in the L ligand can

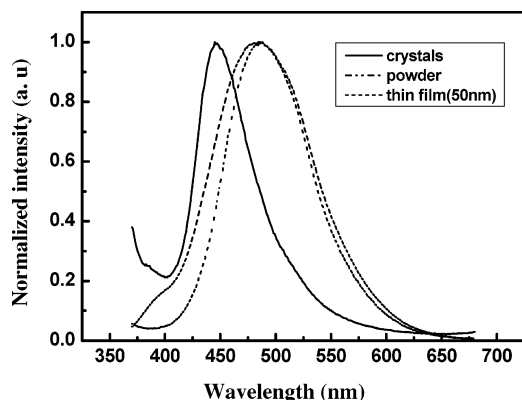


Figure 8. Fluorescence spectra for various **3** systems including powder, a thin film on quartz (thickness 50 nm), and crystals (excitation energy 350 nm).

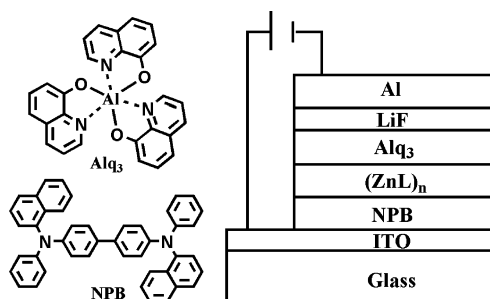


Figure 9. Molecular structures used for EL device fabrication and configuration of the device [ITO/NPB (60 nm)/(ZnL)_n (30 nm)/Alq₃ (30 nm)/LiF (1 nm)/Al (200 nm)].

lead to the change of π and π^* electron orbital levels and sequentially the different excited states in the crystal, solid thin film, and powder phases.

The electroluminescent (EL) properties of (ZnL)_n were investigated. The EL devices were grown on glass, which was precoated with indium tin oxide (ITO) and fabricated by high-vacuum (5×10^{-6} Torr) thermal evaporation techniques. The device structure consists of a layer of hole-transporting material, *N,N'*-bis(α -naphthyl)-*N,N'*-diphenyl-1,1'-biphenyl-4,4'-diamine (NPB), a layer of emitting material (ZnL)_n, and a layer of electron-transporting material tris(8-hydroxyquinolinato)aluminum (Alq₃). Figure 9 shows the molecular structures of materials used in this study and the structure of the device. The EL device structure is [ITO/NPB (60 nm)/(ZnL)_n (30 nm)/Alq₃ (30 nm)/LiF(1 nm)/Al (200 nm)]. The EL spectrum of the device is identical with the PL spectrum of the solid thin film and is shown in Figure 10. This result indicates that the origin of a greenish-blue emission with CIE coordinates of $x = 0.25$ and $y = 0.40$ is attributed to the intrinsic emission of the zinc complex. Figure 11 shows the current–voltage and luminance–voltage characteristics of the device. The turn-on voltage of the device is 5.5 V, and the maximum luminance is 505 Cd/m² at a driving voltage of 13.5 V.

Conclusions

A centrosymmetric dinuclear copper(II) complex and tetranuclear copper(II) and zinc(II) complexes can be prepared on the basis of tridentate ligand L. The synthesis and

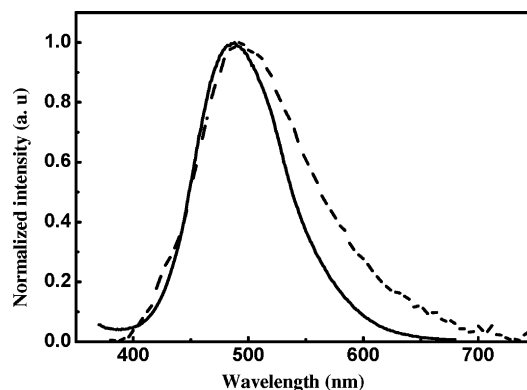


Figure 10. Comparison of the PL spectra of **3** thin film on quartz (thickness 50 nm) and EL spectrum of **3** based on the device [ITO/NPB (60 nm)/(ZnL)_n (30 nm)/Alq₃ (30 nm)/LiF (1 nm)/Al (200 nm)].

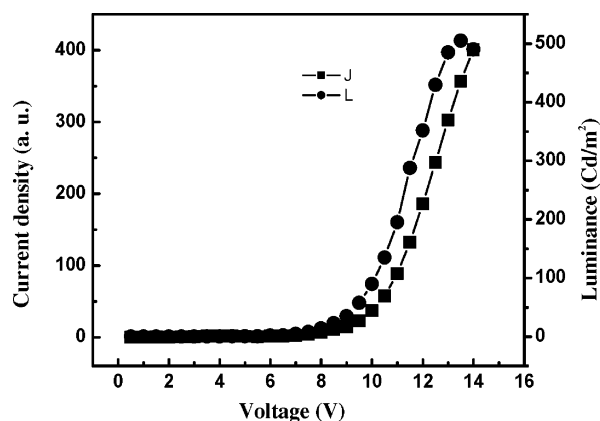


Figure 11. I – V (■) and L – V (●) characteristics for the device [ITO/NPB (60 nm)/(ZnL)_n (30 nm)/Alq₃ (30 nm)/LiF (1 nm)/Al (200 nm)].

structural characterization of the complexes have been presented. In the course of preparation of the dinuclear and tetranuclear complexes, there were revealed different coordination modes. In solid **1**, the two Cu ions having the same coordination environment contain a square-planar Cu₂(μ -O₂) core, while, in solid **2** and **3**, the four ions assuming two different coordination geometries form a set of three adjoining, four-membered Cu₂(μ -O₂) and Zn₂(μ -O₂) rings, respectively. The intermolecular π – π interactions of L ligands on adjacent molecules via pyridyl/pyridyl or pyridyl/phenyl ring overlap and the weak intermolecular hydrogen bonds involving C–H groups and phenolate oxygen atoms from neighboring molecules contribute to the crystal packing of **1** and **2**, which results in the formation of the two- and three-dimensional molecular arrangement. The structure of complex **3** shows that, in contrast to **1** and **2**, the preferred crystal packing involves both close inter- and intramolecular π – π interactions of ligands on adjacent molecules via pyridyl/phenolate ring overlap and results in one-dimensional molecular chains. Crystal **3** and (ZnL)_n exhibit blue and blue-green emission, respectively. The photoluminescence and electroluminescence studies demonstrate that **3** and (ZnL)_n are viable options for potential use as emitting materials in organic electroluminescent devices (OLEDs).

Acknowledgment. This work was supported by the National Natural Science Foundation of China (Grants 50225313 and 50520130316), the Major State Basic Re-

Metal Complexes with Phenoxo Bridges

search Development Program (Grant 2002CB613401), and the Program for Changjiang Scholars and Innovative Research Team in University (Grant IRT0422).

Supporting Information Available: Crystallographic data in CIF format have been deposited with the Cambridge Crystallographic Data Center, CCDC Nos. 283180–283182 for compounds

1–3. Copies of this information may be obtained free of charge from the Director, CCDC, 12 Union Road, Cambridge CB2 1EZ, U.K. (fax, +44-1223-336033; E-mail, deposit@ccdc.cam.ac.uk; <http://www.ccdc.cam.ac.uk>). This material is available free of charge via the Internet at <http://pubs.acs.org>.

IC051531X